# Density measurements in the boundary layer of the ASDEX RF heated plasma

M. EL SHAER*

IPP III/118 November 1986

MAX-PLANCK-INSTITUT FÜR PLASMAPHYSIK

8046 GARCHING BEI MÜNCHEN

MAX-PLANCK-INSTITUT FÜR PLASMAPHYSIK

GARCHING BEI MÜNCHEN

# Density measurements in the boundary layer of the ASDEX RF heated plasma

M. EL SHAER*

IPP III/118 November 1986

* permanent address: Faculty of Engineering,
EL ZAGAZIG University, EL ZAGAZIG, EGYPT

*Die nachstehende Arbeit wurde im Rahmen des Vertrages zwischen dem Max-Planck-Institut für Plasmaphysik und der Europäischen Atomgemeinschaft über die Zusammenarbeit auf dem Gebiete der Plasmaphysik durchgeführt.*

# Density measurements in the boundary layer of of the ASDEX RF heated plasma

M. EL SHAER

Abstract

The boundary layer in the main chamber of ASDEX is diagnosed using a movable 2.2 mm microwave interferometer.

The measured radial density profile decreases exponentially outside of the separatrix with three different e-folding lengths, the middle part of the profile is flatter with a larger e-folding length.

The boundary density increases proportionally to the increase of the main plasma density near the separatrix, far from the separatrix this increase is weaker.
The boundary density increases with the increase of the main magnetic field in the discharge.

With the application of the RF heating at the lower hybrid frequency the boundary density is submitted to a large modification. The behavior of this modification in the density profile depends on the rate of injection of the cold feeding gas. In the discharge with a constant or decreasing gas feeding rate the density profile flattens, and with an increasing rate it steepens when the RF pulse is applied.

## I. Introduction

The measurements of the electron density in the boundary layer of a Tokamak can help to get important informations about the decay of the plasma from the limiter or the separatrix and up to the walls. The parameters of the boundary layer are largely influenced by the change in the main plasma parameters as the main density, the plasma current, the magnetic field and the additional heating.

A movable 2.2 mm microwave interferometer has been installed near the boundary of the ASDEX main chamber facing the Grill coupler in order to investigate the behavior of the density in this region under diffrent conditions.

## II. Experimental arrangement of the microwave interferometer

ASDEX is a Tokamak with a poloidal divertor /1/ having as major radius R = 1.65 m and as nominal minor radius a = 0.40 m. The main magnetic field $B_T \leq 2.8$ T, and the plasma current $I_P \leq 500$ kA. The region investigated in this report is the region between the separatrix radius $r_s$ and the wall in the main chamber, the divertor scrape-off layer measurements are described elsewhere /2/.

The microwave interferometer is mounted on the same toroidal position as the LH Grill coupler, the sending and receiving horns are placed above and below it.

As shown in FIG.1, the two horns can be moved from a large radius R = 2.05 m, which is nearly the separatrix radius for a centered plasma, up to a radius of R = 2.13 m.

The movable horns are connected to the fixed supports, containing the microwave circuit and the power supply by means of flexible teflon parts having as cross section the dimensions of the inner part of the fundamental mode wave-guide, and a sufficient length to assure the motion. The two-tapered extremities of this teflon wave-guide are inserted along a distance of 1.5 cm into adapting small horns from each side.

This method of using the teflon as a flexible wave guide has already been used /3/ and shows very good transmission properties.

The horn used is a non-focusing horn of the pyramidal type with a rectangular aperture of dimensions 23 x 18.8 mm, the height of the horn is 82 mm. At the frequency used, the horn dimensions are calculated for an optimum horn.

The vertical distance between the horns varies, due to the access limitation, between 68 cm for the position close to the separatrix and 78 cm, 8 cm away from it.

The interferometer circuit is built as an unmodulated interferometer /3/, /4/. The microwave signal emitted from an extended interaction oscillator (E.I.O) at a frequency of 136 GHz and a power of $\leq$ 20 W is devided into two parts, one crossing the plasma and the other going through an external reference way.

The phase-detector arrangement is essentially made of two pairs of diodes, each one connected to a mixer having as input the transmitted and the reference signals, the output signals measured by the two diodes are fed into a differential amplifier. Between the two mixers a phase shift of $\pi/2$ has been set. When we plot the output signals coming from the two differential amplifiers on an X-Y display, the result is a point. In the case of a time varying electron density, this point rotates and describes a circle on the condition that the level measured on the four diodes is in equilibrium.

Using a computer program, the phase shift $\Delta\phi$ due to the density variation can be calculated; this is done by taking the arc-tangent of the projection of the circulation point at a certain time on two axis X and Y.

The line density can be calculated using the relation:

$$\int n(e \cdot cm^{-3})\, dl(cm) = 118.4\, f(Hz)\, \Delta\phi(radian)$$

where f is the oscillator frequency, dl is the differential element along the rays path.

## III. Special considerations for the calculation of the density measured by microwave interferometry in the boundary layer of the Tokamak

As a result of the steep density gradient in the boundary layer of a tokamak in combination with the relatively high value of the density near the separatrix, the microwave beam may be deviated due to ray refraction.
This leads to a lower signal on the receiving horn and to an undetermination in the measurement location.

An attempt to estimate the effect of the refraction in the boundary layer is shown in FIG.2 for two cases, one close to the radius of the separatrix and the other 3 cm outside of it. In this calculation the density profile inside the separatrix has the form $n = n_{eo}(1-(x/a)^2)$, where $n_{eo}$ is the density on the axis. The density on the separatrix $n_s$ is assumed to be one-tenth of the peak density $n_{eo}$. Beyond the separatrix the plasma density decreases exponentially with the form

$$n = n_s \exp(-(x-x_s)/\lambda_n)$$

$x_s$ is the separatrix radius and $\lambda_n$ is the density e-folding length.

For the case shown in FIG.2, the peak density is taken to be $5\ 10^{13}$ $cm^{-3}$ so that $n_s$ will be $5\ 10^{12}$ $cm^{-3}$. The profile in the boundary is composed from four steps of different $\lambda_n$, the values of $\lambda_n$ are 2, 4, 2 and 1.5 cm up to the distances 2.5, 3.5, 5 and 10 cm from the separatrix respectively.

From FIG.2 we deduce that near the separatrix the rays are deviated from a straight line connection between the two horns by a distance of 2 to 3 cm in the direction of higher density. However, with the horns positioned 3 cm outside the separatrix, this deviation becomes rather small due to the lower density which reduces the effect of the density gradient on the ray-trajectory.

For the determination of the radial density in the equatorial plane from the measured line averaged density, the following procedure is used: The boundary plasma is assumed to be formed from concentric shells, the density decay between one shell and the other is taken to

be exponential so that the integrated line density can be written as

$$\int_{-l}^{l} ndl = 2\, n_o \int_{o}^{l} \exp(-(x-x_o)/\lambda_n)dl$$

l is the distance between the axis and the outer shell crossing the horn position, $n_o$ is the density at the radius $x_o$, the boundary layer is divided into four regions with different e-folding lengths $\lambda_n$. The density on the separatrix $n_s$, the four values of $\lambda_n$, and the radii of the four shells are assumed. Then we calculate for the assumed values, using a computer program, the line-integrated density profile. The value of $n_s$, the four values of $\lambda_n$ and the width of the four regions $\Delta x$ are then adjusted in order to reproduce the measured line-integrated density profile.
Those values are taken to calculate the radial density profile on the axis. The integration is performed along the straight line connecting the two emitting and receiving horns. Ray refraction is thus not included.

For practical reasons we calculate an equivalent length $\bar{L}(x_o)$ at every radius defined by

$$\bar{L}(x_o) = \int ndl/n_o$$

where we divide the measured value of the line-integrated density by the peak value $n_o$ calculated by the previous procedure. This length can be used to calculate the peak density from the measured line density for the case where the conditions were similar and we don't possess the complete integrated density profile.

This calculation does not take into acccount the effect of the refraction. For a complete description one should integrate along the actual rays path, and then correct the position on the axis for the radius at which the measurement was done.

This procedure is relatively complicated to be repeated for every case. However, since we do not consider the effect of the rays refraction, the values of the density near the separatrix will be overestimated. We estimate that this can be a factor of 2-3 while the densities at positions $x_o - x_s \gtrsim 3$ cm will be unaffected.

## IV. Results of the interferometer density measurements in the ASDEX boundary layer

The measured line integrated profile is used to calculate the radial density profile on the axis without taking into consideration the effect of the rays refraction as described in chapter 3.
In the following results the working gas is deuterium and ASDEX is arranged in the divertor configuration.

FIG.3 shows the radial density profile obtained by keeping the horns position fixed and shifting the large plasma radius. This is repeated for another horn position in another shot. Once normalized to the separatrix radius, the two profiles can be superimposed.

The density profile shown in FIG.3 can be considered to be formed by many steps along the radius. Usually, when going from the center to the boundary plasma a change in $\lambda_n$ is expected at the separatrix radius. This fact can be used to estimate the actual ray deviation due to refraction for the case when the ray touches the separatrix. This occurs when the horns are located some distance outside the separatrix. In FIG.3 we see that this distance is about 1.8 cm. One should take into consideration that for radius $x_o - x_s \gtrsim 3$ cm the profile is unaffected. However, for $x_o - x_s \lesssim 3$ cm, due to the rays bending, the microwave-received signal comes from regions more inside the plasma where the density is higher, the actual density profile inside a radius of 3 cm from the separatrix radius should be flatter than what is reported in FIG.3.

After this first change in $\lambda_n$ we find, when going further in the direction of the wall, that the profile flattens 3.4 cm from the separatrix with a very large $\lambda_n$ of the order of 14 cm which expands along 1.2 cm, and then the profile steepens again with $\lambda_n$ equal to 2.7 cm.

This form of the density profile is not related to a density regime or to special shot conditions; it seems to be a characteristic of the density in the boundary region of ASDEX.
The same flattening is observed in FIG.4 where the density profile is measured for two different mean plasma densities by moving the

horns shot by shot in two reproducible series made at two different large radii. When normalised to their respective separatrix radius, the two profiles have their flat part in the middle of the profile, approximately at the same radius from the separatrix.

The existence of many decay lengths in the density profile measured in the ASDEX boundary layer has already been remarked in the measurements using the Li beam diagnostic and the double probes /6/, /7/. It has been attributed to be a property of the ASDEX divertor configuration. This flattening should be related to the diffusion of the plasma from the main chamber to the divertor and its recombination on the recombination plates there. From those preliminary measurements we can say that the location of this flat part follows the change in the separatrix position and depends mainly on the configuration in the divertor chamber.

The density in the boundary layer of the main plasma chamber and in the divertor chamber is mainly produced by the expansion of the main plasma across the separatrix, perpendicularly to the magnetic field to reach the wall and axially along the field lines to reach the divertor.

The dependence of the boundary plasma density on the main average plasma density is shown in FIG.5 for two different horn positions, 2.4 cm and 8.2 cm from the position of the separatrix. In the region far from the separatrix and for main average densities up to $10^{13}$ $cm^{-3}$, this dependence is nearly linear. In the region between 1 and 2 $10^{13}$ $cm^{-3}$ it becomes flatter which means that the increase in the main average density leads only to a small increase in the boundary density. This can be due to the profile shape. However, near the separatrix the boundary density increases proportionally to the mean central density.

The change in the magnetic field affects the density in the boundary. This is shown in FIG.6. The density increases with the increase of the magnetic field. This is consistent with the reduction of the cross field diffusion. At high magnetic field the loss rates of the particles going to the wall and to the divertor to be recombined there is reduced, making the density higher.

The dependence of the boundary density on the plasma current is shown in FIG.7 for a position 6.3 cm from the separatrix. At this position far from the separatrix, the density decreases with the increase of the plasma current.

Some discrepancy appears in the previous curves, for example between Figures 4 and 5. This occurs between shot series having the same parameters as well as the same mean central density. However, for the same mean density, the density profile in the main plasma can be different leading to different boundary values. The boundary conditions are also influenced from one day to another by the wall conditions and the vacuum quality.

## IV. Modifications in the density profile due to the application of the lower hybrid heating (LHH)

The shape of the density profile in the boundary layer of a Tokamak is an important parameter in understanding the mechanism of heating and coupling of the wave at the lower hybrid frequency.

The RF coupler used in ASDEX is an 8-wave-guide Grill working at a frequency of 1.3 GHz. The characteristics of the heating system are described in Ref. /9/. The Grill position in the following measurements was kept constant at a radius of R = 2.125 m.

An attempt to explain the density variation during the LHH is made considering a new parameter which is the variation in the amount of the feeding gas injected in the discharge during the RF pulse with respect to the normal gas rate.
FIG.8 shows two similar shots measured at a distance of 4 cm from the separatrix; the main density was nearly constant before the application of the RF with a value around $1.1\ 10^{13}\ cm^{-3}$, the gas used was deuterium and the RF power was in the range of 500 KW.

For those two shots the feeding gas valve was programed to maintain the same value of the average main density. In the case A in FIG.8 the gas injection rate was nearly constant. During the RF, however, the density in the boundary layer increases. In the case B a small decrease in the main average density (approximately 2 %) due to the

application of the RF leads to an increase in the gas puffing rate and a decrease in the boundary plasma density. The two shots shown in FIG.8 are made for two different Grill phases. For both shots the power spectrum was symmetric, however for shot A we had $\langle N_{\parallel} \rangle = 4$ while for shot B we had $\langle N_{\parallel} \rangle = 2$. This may explain the different behavior of the main plasma during the RF but is not sufficient to explain directly the density variation in the boundary, which is altered indirectly due to this phase variation.

The modification of the boundary density during RF depends on the shape of the density profile and on the absolute value of the density at a certain radius.
For the case of constant or slightly decreasing gas inlet FIG.9 shows the density profiles with and without RF for a series of shots made at the same mean density, and the Grill operating in the $oo\pi\pi$-mode. The density on the axis is calculated from the line integrated density as described in section 3.

The application of the RF, as seen in FIG.9, results from an increase in the density for low density values and a decrease for high values near the separatrix, the resulting effect being a flattening in the density profile. For the same feeding gas conditions at lower main density and a Grill in the current drive mode ($\Delta\phi = \pi/2$), FIG.10 shows the same effect of flattening of the density profile during the RF.

For the low density part, FIG.11 illustrates the increase in density due to a multistep RF pulse. The density variation is found to follow the RF signal.

The situation is different when an excess amount of cold gas is injected during the RF as a result of a small decrease in the main average density to satisfy the feed-back control of the average density. An example of this case is illustrated in FIG.12 where the density in the boundary is plotted against the main average density. The measurements were done at 5 cm outside the separatrix. For low main density less than $1.3\ 10^{13}\ cm^{-3}$, the RF results on a decrease of the boundary density, for higher densities the tendency is reversed to an increase.

The phenomenon of density variation during the RF in the boundary can be summarized as follows; for a constant gas puffing rate before and after the RF pulse, the density incrases in the boundary for lower values near the wall and decreases for higher values near the separatrix when we apply the RF. This results in a flattening of the profile facing the antenna.
For an excess gas-inlet during the RF due to a feedback controlled main average density, the boundary density decreases for lower values near the wall and increases for higher values near the separatrix with the application of the RF. This results in a steepening of the radial density profile facing the antenna.

The toroidal dependence has not been investigated, all the measurements are done diretly facing the antenna.

Such density varations during the RF in the boundary layer have previously been noted /7/, /8/ and /10/. The interpretation of such phenomena is rather complicated due to the dependence of the boundary density on the different parameters of the discharge; we will limit ourselves to the interpretation, evocating the variation of the neutral gas-feeding rate during the RF, which controls the transport in this region.

The variation of the gas-injection rate may affect the neutral particle concentration in the boundary and also the electron temperature /11/.
From previous measurements with the Langmuir probes in ASDEX /7/ it has been found that the application of the RF results in an increase of the electron temperature near the Grill from 3 to 8 eV. This increase becomes smaller when going toward the separatrix. Such increase is sufficient to produce a higher ionization, knowing that the rate of ionisation by eletrons increases by a factor of 10 in this range /11/.

Considering now the first case, when the gas-injection rate is constant along the discharge before and during the RF and the main average density unchanged, the increase in density near the wall during the RF can be attributed to the ionisation of the neutral particle existing already in the boundary due to the increase in the electron energy directly caused by the RF heating. When going toward

the separatrix the increase in temperature due to the RF becomes smaller, and the ionisation is not enhanced. However, the electron temperature is locally still higher than in the case of the absence of the RF. If we suppose that there is no change in the energy content in the boundary due to the RF, a small increase in the temperature will locally be accompanied by a decrease in the density in order to maintain the same plasma pessure along a toroidal flux line.

In the second case described in FIG.12 a cold neutral gas has been injected into the discharge as a result of a small decrease in the main average density to satisfy the feedback control of this density. The introduction of a cold gas may reduce the boundary electron temperature attenuating the increase due to the RF, so that the relative increase in the temperature will not be sufficient to produce new particles by ionisation. However, it will result in a decrease in the electron density for the same reason as before - to maintain the same plasma pressure along a toroidal line supposing always that there is no energy excess in the boundary due to the RF. If we go now further inside the plasma toward the separatrix, the penetration of the cold gas will be reduced, this temperature "cooling" caused by the cold gas will be minimised, so that the ionisation can take place again increasing the density in this region.

So there is a competition between the energy gained by the electrons in the RF tending to ionise new particles of the neutral gas and the effect of the introduction of a cold neutral gas on the particle balance and transport in this region.

Unfortunately the electron temperature was not systematically measured during those series of shots. However, we refer to previous measurements realized under the same conditions /7/.

Many other effects can be involved in the explanation of such effects like the radiation pressure and the parametic decay instabilities. These effects are, however, more difficult to be evaluated and to be locally measured.

## V. Conclusion

A 2.2 mm microwave interferometer has successfully been used to measure the density in the ASDEX boundary layer. For a reasonable density range the microwave signal hardly suffers from the rays refraction.

The measured density radial profile expands out of the separatrix with three e-folding lenghts, with a flat part in its middle region. The position at which this flat part occurs is independent of the geometrical dimensions of the vessel and depends only on the separatrix position.

The density in the boundary increases proportionally to the main plasma density. Far from the separatrix, however, this dependence becomes weaker for a main density range between $1.10^{13}$ and $2.10^{13}$ $cm^{-3}$.

In the boundary the density increases with the increase of the magnetic field, and far from the separatrix the increase of the plasma current leads to a decrease in the density.

The modifications in the boundary density produced during the application of the lower hybrid heating is found to depend on the amount of the cold gas injected in the discharge.
For a constant gas-feeding rate the density profile flattens with the application of the RF and steepens for an increasing gas-feeding rate.

Acknowledgement

I very much appreciate the interest of Dr. F. Leuterer devoted to this work. The contribution of G. Ichtchenko (CEN Grenoble) was essential for the preparation of this work. I am grateful to Dr. V. Mertens for the ray tracing calculations and to Dr. H.A. Claassen (KFA Jülich) for helping in the numerical integration.

I thank the members of the ASDEX and LH groups for the pleasant atmosphere of work. The support of CEN Grenoble was essential for this work.

References

/1/ M. Keilhacker et al. "Impurity control experiments in the ASDEX Divertor". Proc. 8th Int. Conf. on Plasma Physics and Contr. Fus.Research, Brussels, Vol. II, IAEA, Vienna (1981) 3 51.

/2/ U. Dite, T. Grave, Report IPP III/102, December 1985.

/3/ J.A. How, F. Leuterer and M. Tutter, International Journal of Infrared and Millimeter Waves, Vol. IV, No. 3, 1983.

/4/ M.A. Heald, C.B. Wharton "Plasma Diagnostics With Microwaves", John Willey & Sons.

/5/ D. Groening and N. Gotardi, E. Rossetti, Report IPP III/41, May 1978.

/6/ K. McCormick et al., Rev. Sci. Instrum. 56(5), May 1985, p. 1063.

/7/ M. El Shaer, Report IPP III/96, April 1984.

/8/ M. ElShaer, G. Ichtchenko, Report Eur.CEA.FC 1197, (1983).

/9/ D. Eckhartt et al., Int. Conf. on Heating in Toroidal Plasma, Rome, Proc. of the 4th Int. Sympos. on Heating in Toroidal Plasmas, Roma, March 21 - 28, 1984, p. 501.

/10/ Piricoli Ridolfini "Plasma Physics and Controlled Fusion", Vol. 27, No. 6, PP 709 (1985).

/11/ G.M. McCracken, P.E. Stott, Nucl. Fus., Vol. 19, No. 7 (1979).

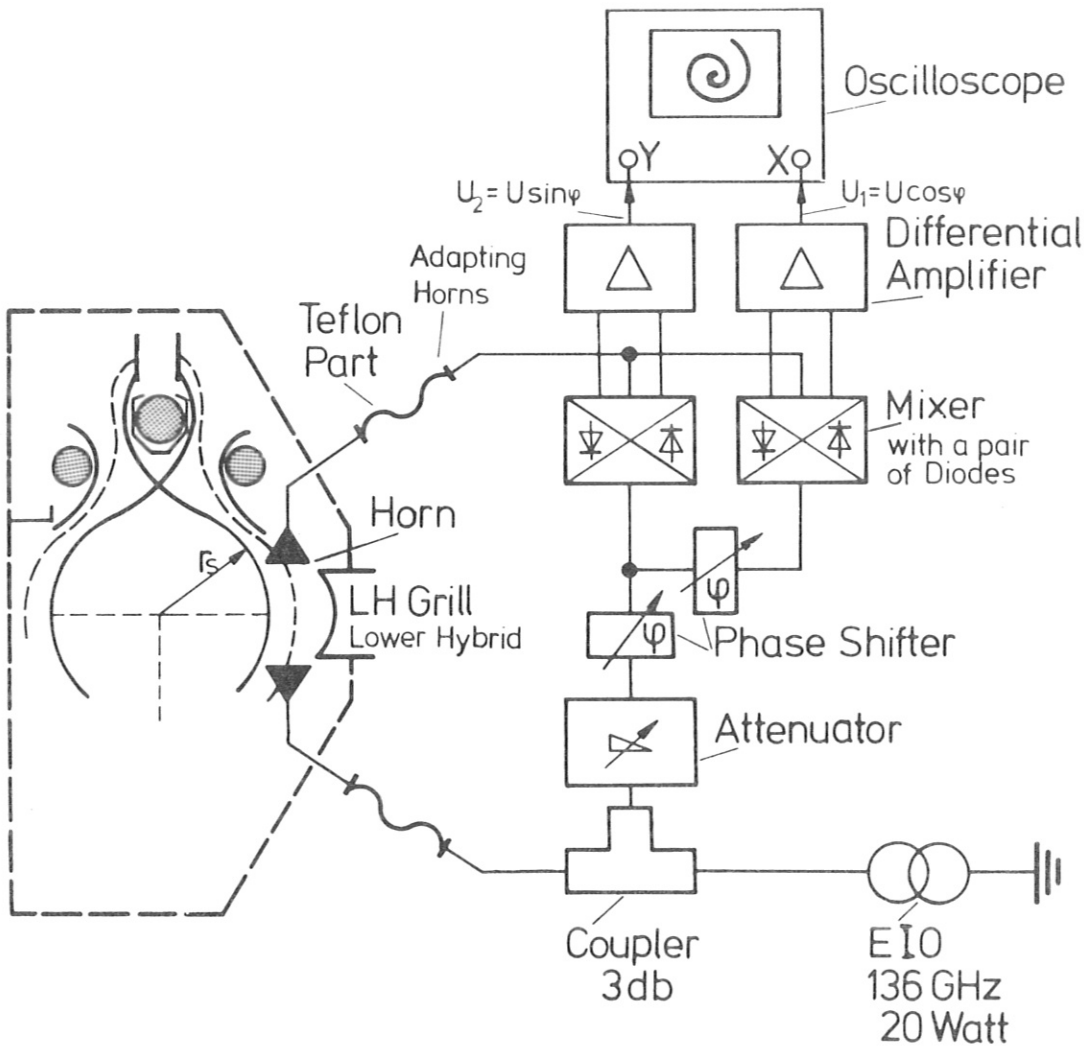


INTERFEROMETER SET UP

Fig. 1: Interferometer set-up

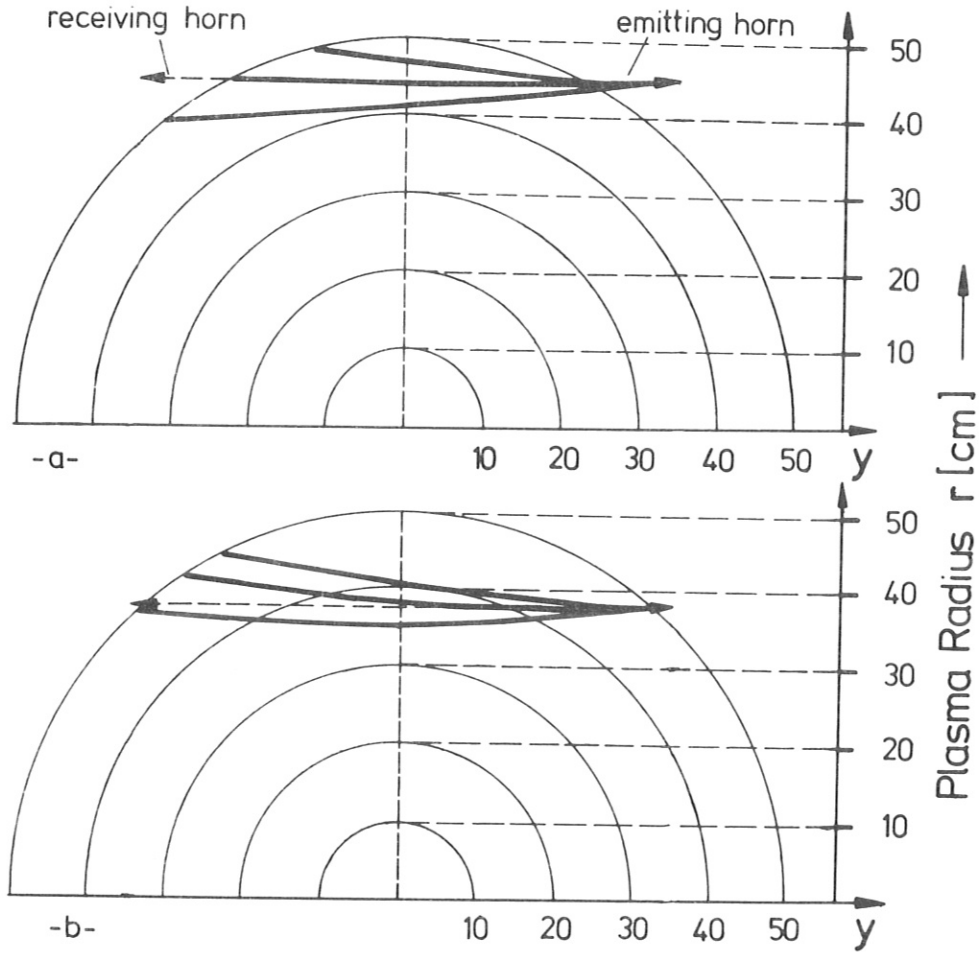


Fig. 2: Ray tracing showing the effect of refraction for a peak density of 9 $10^{13}$ $cm^{-3}$, and separatrix density of 9 $10^{12}$ $cm^{-3}$ placed at $r_s$ = 40 cm

a - outside the separatrix at 43 cm

b - inside the separatrix at 39 cm

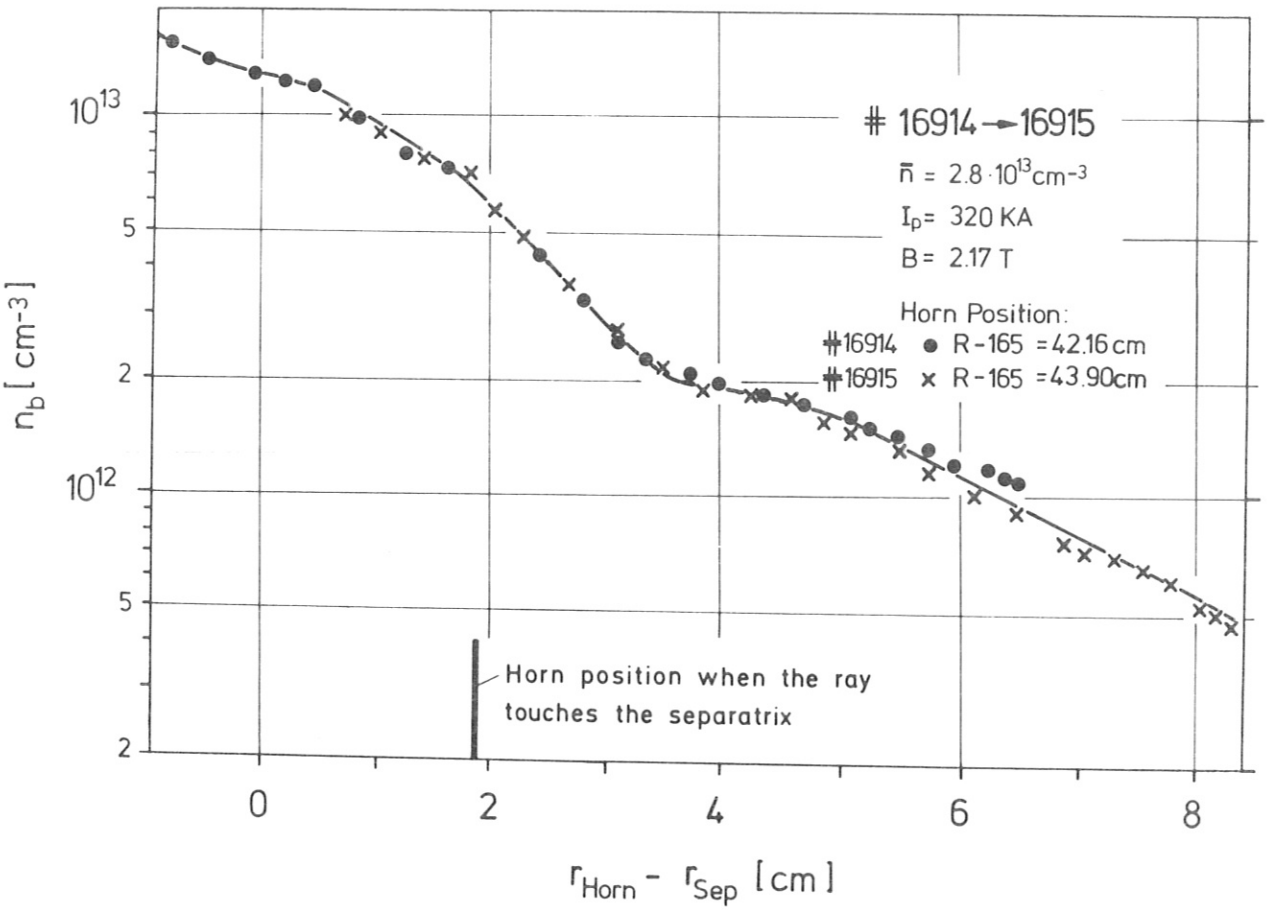


Fig. 3: Density profiles obtained in two shots at two different horn positions normalized to the separatrix position. The profiles are obtained by shifting the plasma while the horns remained at a constant position.

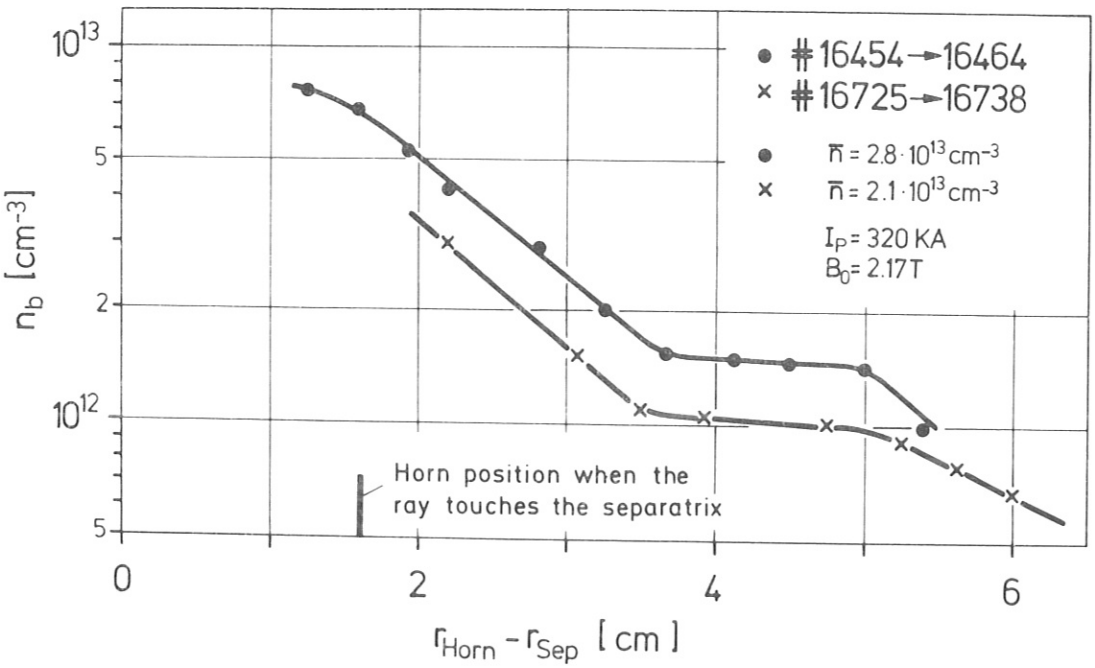


Fig. 4: Density profiles for two different densities normalized to the separatrix position, the two profiles are made shot by shot

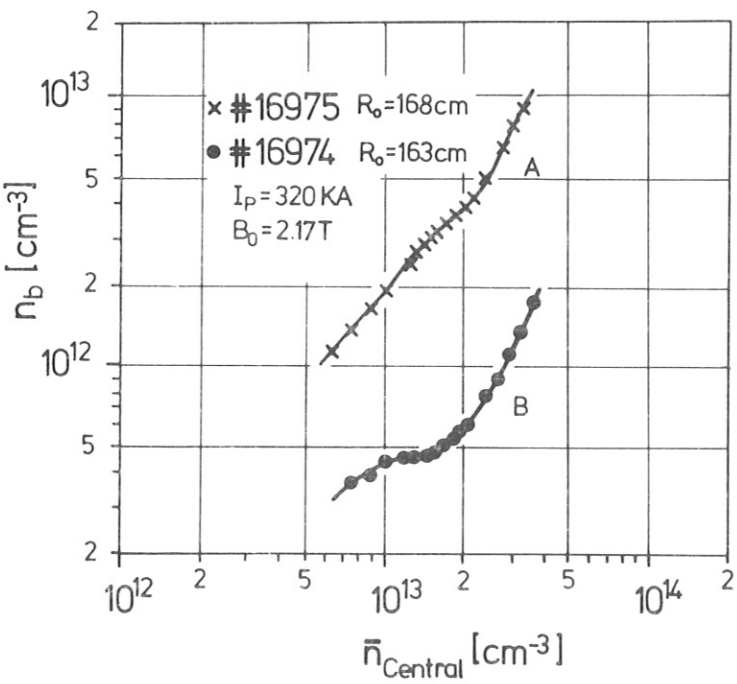


Fig. 5: Dependence of the boundary density, $n_b$, on the main density $\bar{n}$ for two shots having different plasma large radius $R_p$. The horn position (n-1690) = 43.9 cm was kept constant. The distance between the horns and the separatrix is for curves

A = 3.4 cm and

B = 8.2 cm

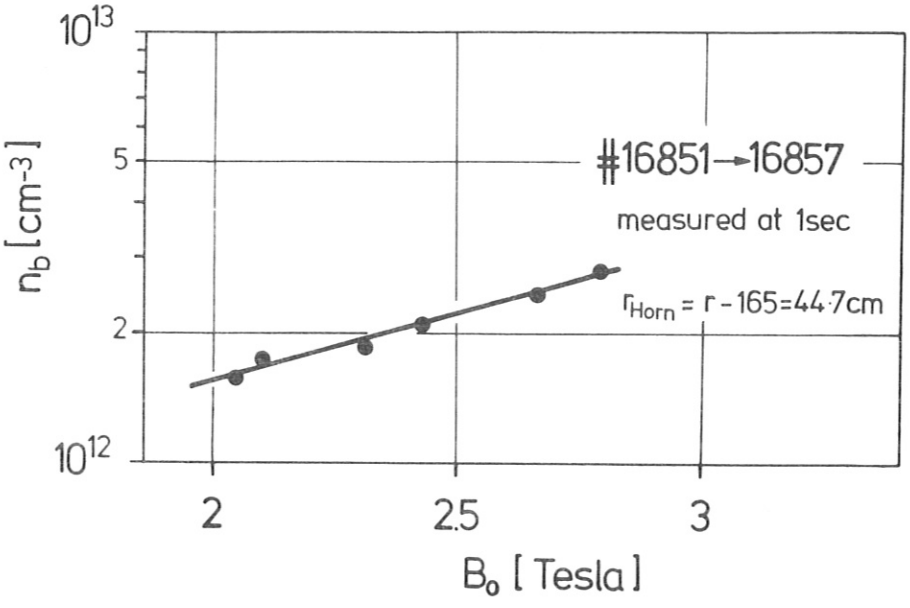


Fig. 6: Dependence of the boundary density on the magnetic field measured at a distance of 6.7 cm from the separatrix.

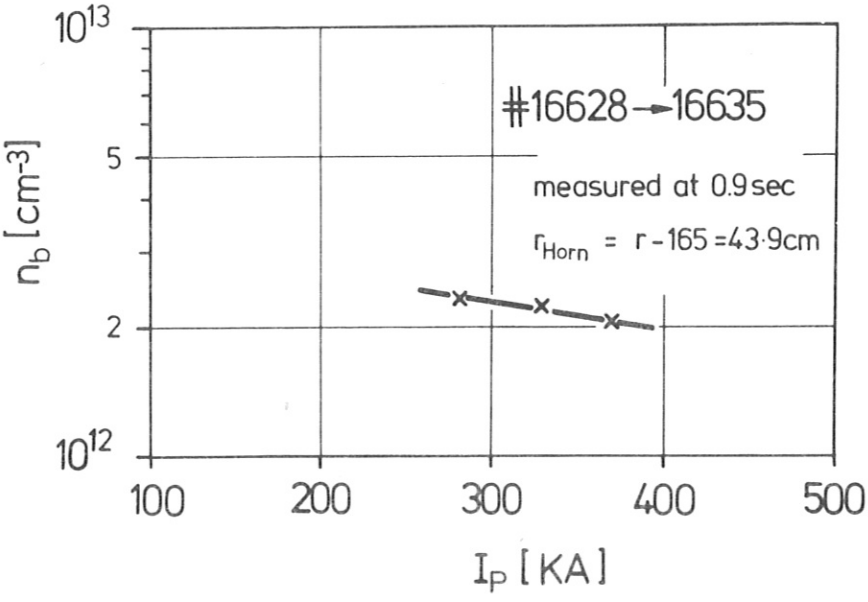


Fig. 7: Dependence of the boundary density on the plasma current measured at a distance of 6.3 cm from the separatrix.

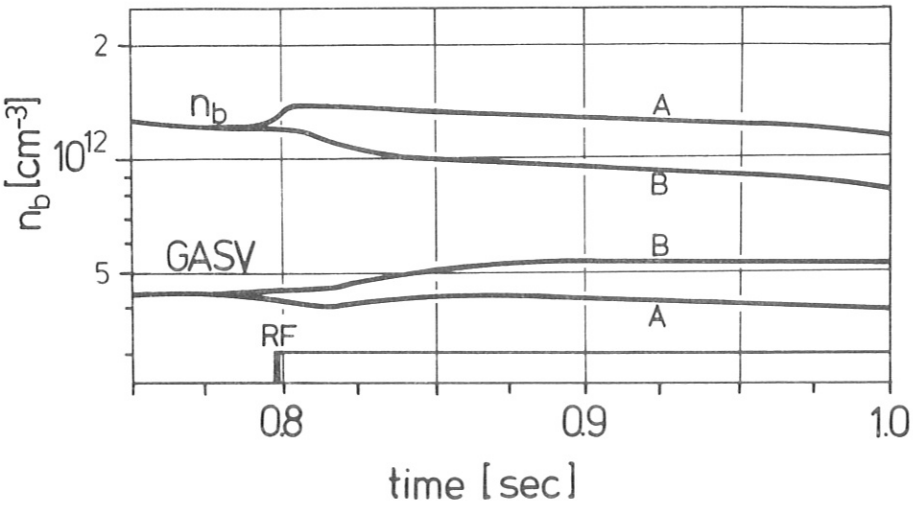


Fig. 8: Boundary density, variations, $n_b$, as a result of the application of the RF heating related to the gas feeding rate, GASV, for:

A: constant gas rate # 15436 Grill phase oo$\pi$o$\pi$

B: increasing gas rate #15437 Grill phase oo$\pi\pi$, $P_{HF}$ 500 Kw mean density $\bar{n}$ = 1.1 $10^{13}$ cm$^{-3}$, measured at 4 cm from the separatrix

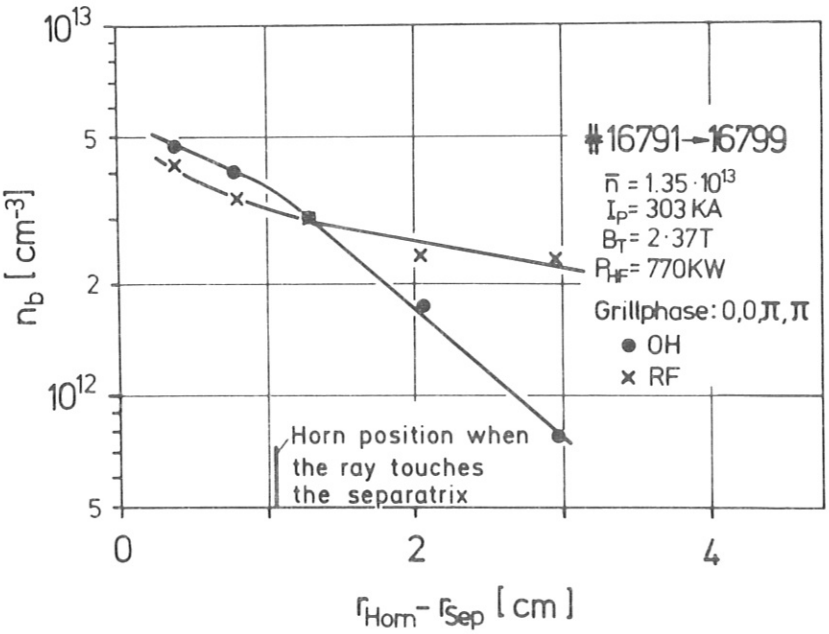


Fig. 9: Density profiles for ohmic and RF heated plasma normalized to the separatrix position.

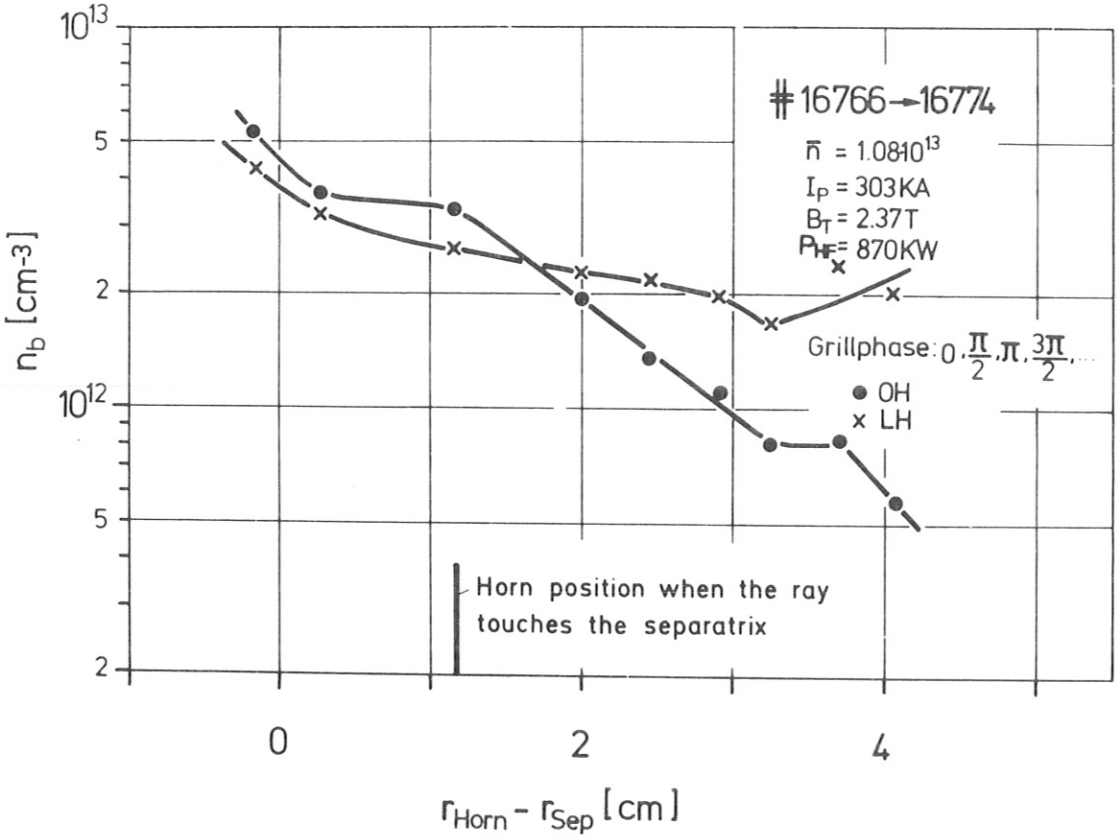


Fig. 10: Density profiles for plasmas with inductive or RF-driven plasma current normalized to the separatrix position.

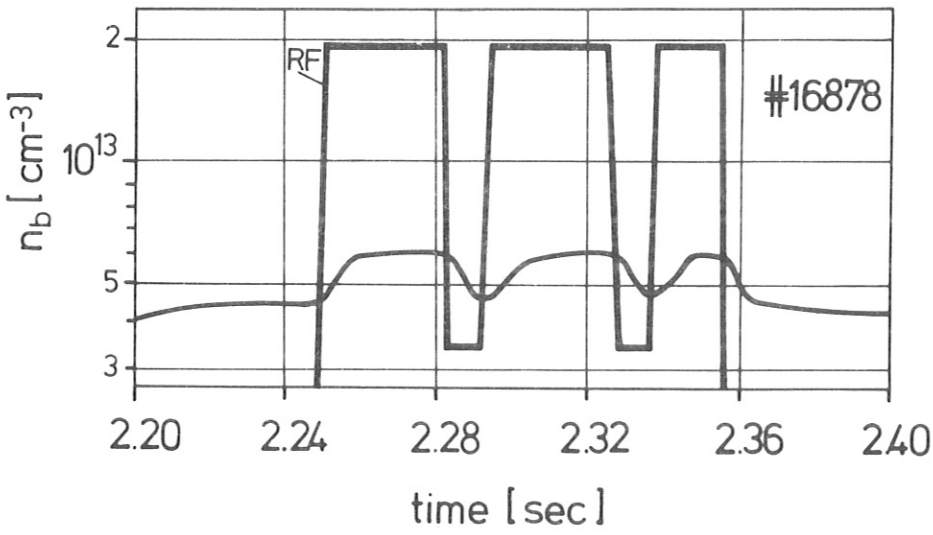


Fig. 11: Density variations for a pulsed RF signal, measured at (r-169) = 43 cm.

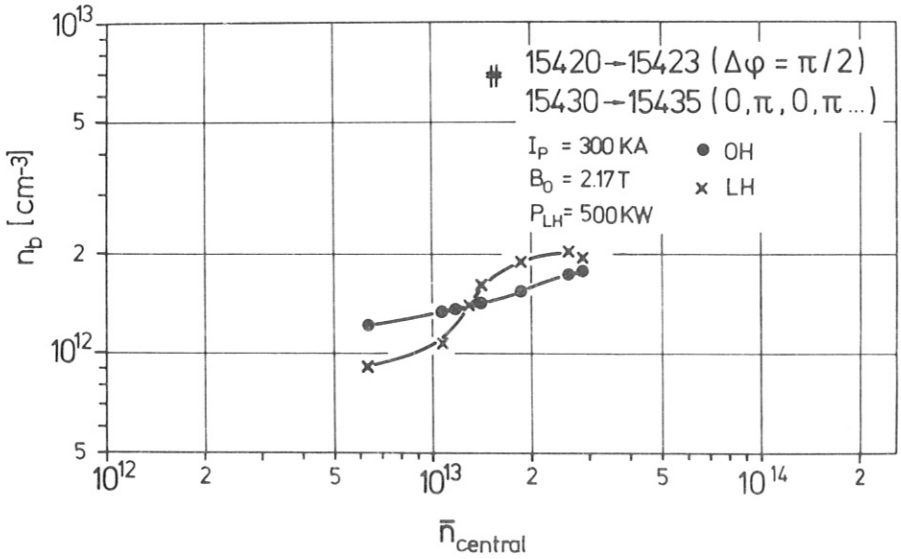


Fig. 12: Dependence of the boundary density on the main density $\bar{n}$, for OH and LH cases. The distance between the horn position and the separatrix is 4 cm.